MolecularMedicine

c-Met Inhibitor Synergizes with Tumor Necrosis Factor–Related Apoptosis-Induced Ligand to Induce Papillary Thyroid Carcinoma Cell Death

Rong Bu,[1*] Shahab Uddin,[1*] Maqbool Ahmed,[1] Azhar R Hussain,[1] Saif Alsobhi,[2] Tarek Amin,[3] Abdurahman Al-Nuaim,[3] Fouad Al-Dayel,[4] Jehad Abubaker,[1] Prashant Bavi,[1] and Khawla S Al-Kuraya[1]

[1]Human Cancer Genomic Research, Research Center; [2]Department of Surgery; [3]Department of Endocrinology; and [4]Department of Pathology, King Faisal Specialist Hospital and Research Center, Riyadh, Saudi Arabia

The Met receptor tyrosine kinase is overexpressed and/or activated in variety of human malignancies. Previously we have shown that c-Met is overexpressed in Middle Eastern papillary thyroid carcinoma (PTC) and significantly associated with an aggressive phenotype, but its role has not been fully elucidated in PTC. The aim of this study was to determine the functional link between the c-Met/AKT signaling pathway and death receptor 5 (DR5) in a large cohort of PTC in a tissue microarray format followed by functional studies using PTC cell lines and nude mice. Our data showed that high expressions of p-Met and DR5 were significantly associated with an aggressive phenotype of PTC and correlated with *BRAF* mutation. Treatment of PTC cell lines with PHA665752, an inhibitor of c-Met tyrosine kinase, inhibited cell proliferation and induced apoptosis via the mitochondrial pathway in PTC cell lines. PHA665752 treatment or expression of c-Met small interfering (si)RNA resulted in dephosphorylation of c-Met, AKT and its downstream effector molecules. Furthermore, PHA665752 treatment upregulated DR5 expression via generation of reactive oxygen species in PTC cell lines, and synergistically potentiated death receptor–induced apoptosis with tumor necrosis factor–related apoptosis-inducing ligand (TRAIL). Finally, cotreatment with PHA665752 and TRAIL caused more pronounced effects on PTC xenograft tumor growth in nude mice. Our data suggest that the c-Met/AKT pathway may be a potential target for therapeutic intervention for treatment of PTC refractory to conventionally therapeutic modalities.
Online address: http://www.molmed.org
doi: 10.2119/molmed.2011.00238

INTRODUCTION

Papillary thyroid carcinoma (PTC) represents 80–90% of all thyroid malignancies worldwide (1) and is ranked second only to breast cancer among females in Saudi Arabia. PTC is usually well differentiated, but the clinical behavior of PTC varies widely (2). The prognosis for PTC is often favorable; however, approximately 20% of PTC tumors recur and some reach advanced stages (3). Several clinicopathological variables, including stage, cancer invasion and distant metastasis, are used for prognostication for PTC (4,5) However, the factors and mechanisms determining the aggressive behavior of some papillary carcinomas that result in recurrence and metastatic lesions refractory to current modalities of treatment are still not fully known.

Therefore, there is a need for further research to elucidate the molecular mechanisms and discover relevant targeted therapies.

Activation of receptor tyrosine kinase (RTK) encoding for the hepatocyte growth factor receptor (c-Met) has been reported in PTC (6). Binding of the receptor to its ligand, hepatocyte growth factor/scatter factor (HGF/SF) induces receptor dimerization, triggering conformational changes that activate Met tyrosine kinase activity (7). Met activation can have profound effects on cell growth, survival, motility, invasion and angiogenesis (8,9). Dysregulation of Met signaling has been shown to contribute to tumorigenesis in a number of malignancies, including thyroid cancer (10). On the basis of these findings, it has been suggested that hepatocyte growth factor (HGF) and its receptor tyrosine kinase c-Met play a crucial role in determining

The Feinstein Institute for Medical Research North Shore LIJ

the invasiveness of PTC cells, and c-Met expression has been found to be associated with the aggressive tall cell variant of PTC (11,12) and a high risk of metastasis (13). We have recently reported that the *c-Met* gene is overexpressed in 37% of PTCs in Saudi patients, and *c-Met* expression was significantly associated with aggressive behavior, for example, higher stage, nodal involvement and tall cell variant (14). Furthermore, 55% of PTC cases express activated AKT (p-AKT), which suggests that p-AKT may play an important role in PTC tumorigenesis. The fact that most of the PTC cases that have activated AKT show overexpression of c-Met suggests that c-Met may be an alternative mechanism of AKT activation in Middle Eastern PTC (14). Furthermore, c-Met dysregulation is associated with aggressive behavior and may serve as a molecular biomarker and potential therapeutic target in this type of cancer (14).

Programmed cell death or apoptosis is a genetically regulated process that plays an essential role in the regulation of homeostasis of higher organisms (15). Aberrant regulation of apoptosis can lead to cancer. Two major pathways that lead to apoptosis exist: the mitochondrion-initiated pathway, also defined as the intrinsic pathway, and the cell-surface death-receptor pathway, also defined as the extrinsic pathway (16). Death receptors are key components in the extrinsic apoptotic pathway. Their activation due to ligand binding or receptor clustering and aggregation triggers an extrinsic apoptotic signaling pathway leading to apoptosis. One example is tumor necrosis factor–related apoptosis-inducing ligand (TRAIL), which is the ligand for death receptor 4 (DR4) and death receptor 5 (DR5) and induces apoptosis upon ligation with DR4 or DR5.

In the present study, we assessed the prevalence of p-Met protein expression and its relation to DR5, activated AKT and its downstream antiapoptotic targets such as XIAP and Bcl-XL in a large cohort of Saudi PTCs using tissue microarray (TMA) technology. We next investi-

gated the antitumor activity of PHA665752, an inhibitor of c-Met activation, against human PTC cell lines. Our data indicated that PHA665752 induces upregulation of DR5 in PTC cells via a mechanism involving generation of reactive oxygen species (ROS). Finally, we also studied the effect of PHA665752 combined with TRAIL on PTC and on xenografts of these cells in a nude mouse model. Altogether, our present findings suggest that the HGF/c-Met signaling pathway is an attractive therapeutic target for PTC that typically shows deregulated c-Met pathways.

MATERIALS AND METHODS

Patient Selection, TMA Construction and Immunohistochemistry

A total of 536 patients with papillary thyroid carcinoma (PTC) diagnosed between 1988 and 2004 were selected from King Faisal Specialist Hospital and Research Centre. Clinical and histopathological data were available for all these patients. All samples were analyzed in a TMA format. TMA construction was performed from formalin-fixed, paraffin-embedded PTC specimens as described earlier (17). The institutional review board of the King Faisal Specialist Hospital and Research Centre approved the study. Tissue microarray slides were processed and stained manually as described previously (14). The primary antibodies used and their dilutions, and incidences are listed in Supplementary Table 1. p-Met and DR5 were categorized by an H score as described previously (18). Overexpression and reduced/absent expression scores for p-Met (H score > 20 = high expression) and DR5 (H score > 220 = high expression) were defined by use of X-tile. XIAP, Bcl-XL and p-AKT scoring were done as explained earlier (19,20).

Cell Lines and Culture Conditions

The PTC cell line B-CPAP was purchased from DSMZ (Braunschh, Germany) and TPC-1 was kindly provided by B McIver (Department of Endocrinology, Mayo Clinic, Rochester, MN, USA)

as a gift, and cultured as previously described (21).

Reagents and Antibodies

PHA665752 was purchased from Tocris Cookson Inc (Ellisville, MO, USA). Super*Killer* TRAIL was purchased from Alexis Corporation (Lausen, Switzerland). Bax (6A7) antibody was purchased from Sigma (St. Louis, MO, USA). Cleaved caspase-3, p-Akt, p-Foxo1, p-GSK3, BID, XIAP, cIAP1, caspase-8 and c-Met antibodies were purchased from Cell Signaling Technologies (Danvers, MA, USA). c-Met, cytochrome c, β-actin, caspase-3 and poly (ADP)ribose polymerase (PARP) antibodies were purchased from Santa Cruz Biotechnology (Santa Cruz, CA, USA). p-Met (Y1230/Y1234/Y1235) antibody was purchased from Invitrogen (Camarillo, CA, USA). Annexin V/propidium iodide was purchased from Molecular Probes (Eugene, OR, USA). The apoptotic DNA-ladder kit was obtained from Roche (Penzberg, Germany). JC1 was purchased from Aexis (San Diego, CA, USA).

3-(4,5-Dimethylthiazol-2-yl)-2,5-Diphenyltetrazolium Bromide Assays

Cells (10^4) were incubated in triplicate in a 96-well plate with or without indicated doses of PHA665752 for 24 h. The ability of PHA665752 to suppress cell growth was determined by 3-(4,5-dimethylthiazol-2-yl)-2,5-diphenyltetrazolium bromide (MTT) cell proliferation assays, as previously described (22).

Annexin V/Propidium Iodide Dual Staining

PTC cell lines were treated with the indicated concentrations of PHA665752. The cells were harvested and the percentage of cells undergoing apoptosis was measured by flow cytometry after staining with fluorescein-conjugated Annexin V and propidium iodide as previously described (23).

DNA Laddering

The DNA laddering assay was performed as described earlier (24). Briefly, cells (2×10^6) were treated with and

without PHA665752 for 24 h. DNA was extracted, and 2 μg DNA was eletrophoresed on 1.5% agarose gel containing ethidium bromide at 75 V for 2 h.

Cell Lysis and Immunoblotting

Cells were treated with PHA665752 as described in the figure legends and lysed as previously described (25). Proteins (10 μg) were separated by sodium dodecyl sulfate–polyacrylamide gel electrophoresis (SDS-PAGE) and transferred to a polyvinylidene difluoride (PVDF) membrane. Immunoblotting was done with different antibodies and visualized by use of the Amersham ECL Western Blotting Analysis System.

Gene Silencing by Using siRNA

DR5, c-Met small interfering (si)RNAs and scrambled siRNA were purchased from Santa Cruz Biotechnology. Cells were transfected by use of Lipofectamine 2000 for 6 h, then the lipid and siRNA complex was removed and fresh growth medium was added. After 48 h, cells were used for apoptosis experimental analysis by flow cytometry or protein level determination by Western blotting analysis.

Detection of Bax Conformational Changes

This assay was performed as described earlier (24). Briefly, after treatment with the indicated reagents for the indicated time points, cells were lysed with Chaps lysis buffer. We then incubated 500 μg of total protein with 2 μg of anti–Bax 6A7 monoclonal antibody for 2 h at 4°C. Then, 25 μL of protein G-beads was added and incubated at 4°C overnight. Following washes in lysis buffer, samples were separated by SDS-PAGE and immunoblotted with N20 Bax polyclonal antibody.

Measurement of Mitochondrial Membrane Potential

After treatment of PHA665752 for 24 h, cells were incubated with 10 μmol/L JC1 at 37°C in the dark for 30 min, and mitochondrial membrane potential (percent-

age of green and red aggregates) was determined by flow cytometry (26).

Assays for Cytochrome c Release

The release of cytochrome c from the mitochondria was assayed as described earlier (19). Briefly, cells were treated with or without PHA665752 as described in the figure legends, and cytosolic and mitochondrial fractions were isolated. We analyzed 20 μg of protein from the cytosolic fraction of each sample by immunoblotting using an anti–cytochrome c antibody.

Measurement of ROS

Exponentially growing cells were pretreated with PHA665752 10 μmol/L for 0, 2, 4 and 6 h, respectively, then loaded with 10 μmol/L H2D*CF*DA. After 45 min incubation at 37°C, the green fluorescence intensity in the cells was examined by fluorescence-activated cell-sorting (FACS) analysis.

Reverse Transcription–Polymerase Chain Reaction Assays

Total RNA was isolated followed by 10 μmol/L PHA665752 treatment for 24 h with or without 10 mmol/L N-acetyl cytsteine (NAC) pretreatment for 2 h by using Trizol (Invitrogen, Carlsbad, CA, USA) and reverse transcribed with random hexamers. Reverse transcription–polymerase chain reaction (RT-PCR) was performed by using the following primers: DR5 forward: GGAAGCCGCTCATGAGGAAGTTGG; DR5 reverse: GGCAAGTCTCTCTCC CAGCGTCTC for 25 cycles (60°C annealing temperature) to produce a 181-bp product. RT-PCR amplification of glyceraldehyde-3-phosphate dehydrogenase (GAPDH) was used as an internal control. All PCR products were analyzed by 4% agarose gel electrophoresis and visualized with ethidium bromide under UV light using an α Imager (α Innotech, San Leandro, CA, USA).

Relative Quantification Analysis by Real-Time RT-PCR

All reactions were done in glass capillaries (Roche) with a final reaction vol-

ume of 10 μL of 1 × LightCycler FastStart DNA Master SYBR Green I reaction mixture (Roche, Mannheim, Germany) containing FastStart *Taq*, reaction buffer, dNTPs (deoxynucleoside-5′-triphosphates), 1 mmol/L MgCl2 and 0.5 μmol/L of each DR5 primer. For each sample, PCR amplification was performed in triplicate. GAPDH was used as an endogenous control. Thermocycling and detection were done on the LightCycler (Roche). The relative expression ratio of a target gene was calculated on the basis of efficiency (E) and crossing point (C_P) deviation of treated cell line versus control (nontreated), and expressed in comparison to a reference gene, *GAPDH* (14).

Animals and Xenograft Study

Six-week-old nude mice were obtained from Jackson Laboratories (Bar Harbor, ME, USA) and maintained in a pathogen-free animal facility for at least 1 wk before use. All animal studies were done in accordance with institutional guidelines. For the xenograft study, mice were inoculated subcutaneously into the right abdominal quadrant with 10×10^6 TPC-1 cells in 200 μL phosphate-buffered saline. After 1 wk, mice were randomly assigned into four groups: three groups receiving 25 μg/kg TRAIL, 25 mg/kg PHA665752 and a combination of 25 μg/kg TRAIL and 25 mg/kg PHA665752 intraperitoneally, respectively, and one remaining group receiving 0.9% saline. The body weight and tumor volume of each mouse was monitored weekly. After 5 wks of treatment, mice were killed and individual tumors were weighed, then snap frozen in liquid nitrogen for storage.

Statistical Analysis

The JMP8.0.2 (SAS Institute, Cary, NC, USA) software package and SPSS 17.0 software (SPSS, Chicago, IL, USA) were used for data analyses. A *P* value <0.05 was considered significant.

*All supplementary materials are available online at www.molmed.org.*

RESULTS

p-Met Expression Is Associated with DR5 in PTC

Levels of p-Met and DR5 (TRAIL-*R*2) were examined by immunohistochemistry (IHC) in a series of 536 PTC and nonneoplastic normal thyroid tissue (Supplementary Figures 1A, B). The incidence of high p-Met and DR5 expression in PTC was 69.9% (314/449) and 23.2% (116/499), respectively. p-AKT activation was significantly higher ($P = 0.0012$) in the PTC subgroup with high p-Met expression (175/224;78.1%) compared with PTC subgroup with low p-Met expression (123/193; 63.7%). Similarly DR5 expression was significantly higher ($P = 0.0062$) in the PTC subgroup with high p-Met expression (85/106; 80.2%) compared with the PTC subgroup with low p-Met expression (221/332; 66.6%). Representative IHC data for both markers were available in 438 TMA spots and were further analyzed. p-Met was not associated with patients' age, sex or disease stage at presentation.

We further stratified all our PTC cases into 4 groups, depending on the presence of p-Met expression and DR5 expression status: high coexpression of p-Met and DR-5 (n = 85); low coexpression of p-Met and DR-5 (n = 111); low p-Met and high DR5 expression (n = 21); and high p-Met and low DR5 expression (n = 221) groups. Of these 4 groups only the 2 subgroups showing direct associations between p-Met and DR5 expression (n = 196) were selected for further analysis. As summarized in Table 1, coexpression of high p-Met and DR5 showed an aggressive phenotype characterized by older age ($P = 0.0004$) and advanced stage ($P = 0.0146$). Interestingly, coexpression of high p-Met and DR5 was also linked to activation of the PI3K/AKT signaling pathway, as is evident from direct significant associations with p-AKT, BCL-XL, XIAP and PIK3CA 110 α subunit protein (p110 α) ($P = 0.0045, 0.0068, 0.0049$ and < 0.0001, respectively). However, coexpression of high p-Met and DR5 did not show any
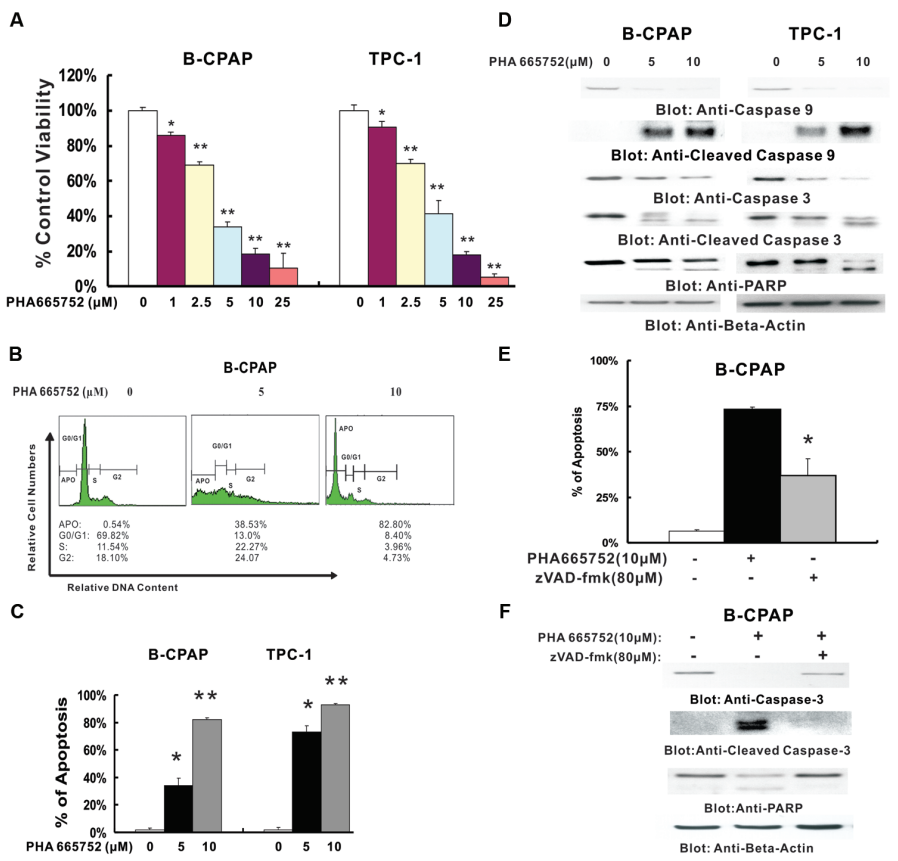
Figure 1. Effect of PHA665752 treatment on cell proliferation and apoptosis in PTC cell lines. (A) PHA665752 inhibits the proliferation of PTC cells. B-CPAP and TPC-1 cells were incubated with 0, 1, 2.5, 5, 10 and 25 μmol/L PHA665752 for 24 h. Cell proliferation assays were performed by using MTT as described in Materials and Methods. Columns, mean of three independent experiments with replicates of six wells for all the doses and vehicle control for each experiment; bars, SD. *$0.001 > P < 0.05$; **$P < 0.001$, statistically significant. (B) PHA665752 causes cell-cycle arrest in B-CPAP cells. B-CPAP cells were treated with 5 and 10 μmol/L PHA665752 for 24 h. Thereafter, the cells were washed and stained with propidium iodide and analyzed for DNA content by flow cytometry. (C) PHA665752-induced apoptosis detected by Annexin V/propidium iodide dual staining. B-CPAP and TPC-1 cells were treated with various doses of PHA665752 (as indicated) for 24 h and cells were subsequently stained with fluorescein-conjugated Annexin V and propidium iodide and analyzed by flow cytometry. Columns, mean of three independent experiments; bars, SD. *$0.05 < P < 0.01$; **$P < 0.001$. (D) Caspase 9 and 3 activation and PARP cleavage following PHA665752 treatment. B-CPAP and PTC-1 cells were treated with and without 5 and 10 μmol/L PHA665752 for 24 h. Cytoplasmic extracts were prepared. Then 10 μg protein from each sample was separated on SDS-PAGE and transferred to PVDF membrane and immunoblotted with antibodies against caspase 9, caspase 3, cleaved caspase 3 and PARP. The blots were probed with an antibody against β-actin for equal loading. (E) Effect of zVAD/fmk on PHA665752-induced apoptosis detected by Annexin V/propidium iodide dual staining. B-CPAP cells were pretreated with 80 μmol/L zVAD/fmk for 2 h and subsequently treated with 10 μmol/L PHA665752 for 24 h, and then cells were stained with fluorescein-conjugated Annexin V and propidium iodide and analyzed by flow cytometry. Columns, mean of three independent experiments; bars, SD. *$P < 0.01$. (F) Effect of zVAD/fmk on PHA665752-induced activation of caspase 3 and cleavage of PARP. B-CPAP cells were pretreated with 80 μmol/L zVAD/fmk for 2 h and subsequently treated with 10 μmol/L PHA665752 for 24 h. Then cells were lysed and equal amounts of proteins were separated on SDS-PAGE and transferred to PVDF membrane, and immunoblotted with antibodies against caspase 3, PARP and β-actin.

Table 1. Clinic-pathological characteristics of p-Met and DR5 coexpression in PTC.[a]

	Total		Both high		Both low		
	No.	%	No.	%	No.	%	P
No. of patients	196		85	43.4	111	56.6	
Age, years							
≤45	102	52.0	32	31.4	70	68.6	0.0004
>45	94	48.0	53	56.4	41	43.6	
Extrathyroidal extension							
Absent	87	44.4	32	36.8	55	63.2	0.0956
Present	109	55.6	53	48.6	56	51.4	
Stage[a]							
I	100	54.3	35	35.0	65	65.0	0.0146
II	11	6.0	3	27.3	8	72.7	
III	19	10.3	13	68.4	6	31.6	
IV	54	29.4	28	51.8	26	48.2	
p-AKT[b]							
High (2–3)	91	50.0	51	56.0	40	44.0	0.0045
Low (0–1)	91	50.0	32	35.2	59	64.8	
PIK3CA-IHC[b]							
High	139	71.7	73	52.5	66	47.5	<0.0001
Low	55	28.3	12	21.8	43	78.2	
BCLXL[b]							
High	50	25.6	30	60.0	20	40.0	0.0068
Low	145	74.4	55	37.9	90	62.1	
XIAP[b]							
High	70	36.1	40	57.1	30	42.9	0.0049
Low	124	63.9	45	36.3	79	63.7	
HGF-1[b]							
High	38	21.0	30	79.0	8	21.0	<0.0001
Low	143	79.0	49	34.3	94	65.7	
[c]5-Year disease-free survival				75.6		65.2	0.9623

[a]Stage information was not available in 12 of the 196 PTC cases with data available for coexpression of p-Met and DR5.
[b]IHC was noninformative in some TMA spots ranging from 1 to 15 indicated in parenthesis: p-AKT (14); PIK3CA, PTEN and XIAP (2 each); BCL-XL (1); HGF-1 (15).
[c]Disease-free survival data were available for some patients but the remaining patients for whom disease-free survival data were not available were excluded from survival analysis.

association with disease-free survival (*P* = 0.9623).

PHA665752 Inhibits Cell Proliferation and Induces Apoptosis in PTC Cells

PHA665752 has previously been reported to affect cell proliferation in various cell lines (27,28). We therefore tested its effect on cell proliferation of PTC cells by MTT assay and determined the doses for further experiments by IC50 (half-maximal inhibitory concentration) of PHA665752. As shown in Figure 1A, as the dose of PHA665752 increased, cell growth inhibition increased in a dose-dependent fashion in both PTC cell lines.

PHA665752-induced growth inhibition was statistically significant (*P* < 0.01) at most of the doses tested. The IC50 values calculated from our graphed results using SPSS 17.0 were 3.92 ± 0.59 μmol/L and 3.84 ± 0.58 μmol/L, respectively, so the doses of 5 and 10 μmol/L were used for further experiments.

In subsequent experiments, we determined whether the observed suppressive effect of PHA665752 in the MTT assay was ascribable to induction of apoptosis. After 24 h of treatment with PHA665752, cell fractions were determined by flow cytometry. As shown in Figure 1B the sub-G1 population of cells increased

from 0.48% in vehicle to 33.3% with 5 μmol/L and 83.96% with 10 μmol/L in B-CPAP cells. Similar results were obtained in TPC1 cells (data not shown). These results indicated that PHA665752 treatment results in apoptosis in PTC cells. PHA665752-induced apoptosis in PTC cells was further confirmed by Annexin V/PI dual staining (Figure 1C and Supplementary Figure 2A) and DNA-laddering methods (Supplementary Figure 2B). These results suggest that suppression of growth by PHA665752 in PTC cells is via induction of apoptosis.

Finally we sought to determine whether PHA665752 induced apoptosis via activation of caspase-9, caspase-3 and cleavage of PARP. Figure 1D shows that PHA665752 treatment led to the activation of caspase-9 and caspase-3 and cleavage of PARP in PTC cells in a dose-dependent manner. Furthermore, PHA665752 treatment resulted in activation of caspase-8, leading to truncation of Bid in both cell lines, as we inferred through the decreased intensity of the full-length Bid band (Supplementary Figure 2D). In addition, pretreatment of B-CPAP with 80 μmol/L z-VAD/fmk, a universal inhibitor of caspases, followed by PHA665752 treatment, abrogated apoptosis in B-CPAP cells (Figure 1E and Supplementary Figure 2C) and also prevented caspase-3 and PARP activation (Figure 1F). These results clearly indicate that inhibition of c-Met by PHA665752 causes apoptosis via activation of the mitochondrial apoptotic pathway in PTC cells.

Constitutive Expression of Met and Activation of c-Met Signaling Pathway in PTC Cells

We first performed an experiment in which the B-CPAP cells were treated with indicated doses of PHA665752 for 4 h. After cells were lysed, Western blot was performed. As shown in Supplementary Figure 3, up to 10 μmol/L PHA665752 treatment did not affect phosphorylaton of Lyn, stat3, Jak2 and Src. These results are consistent with the observation in early studies in which
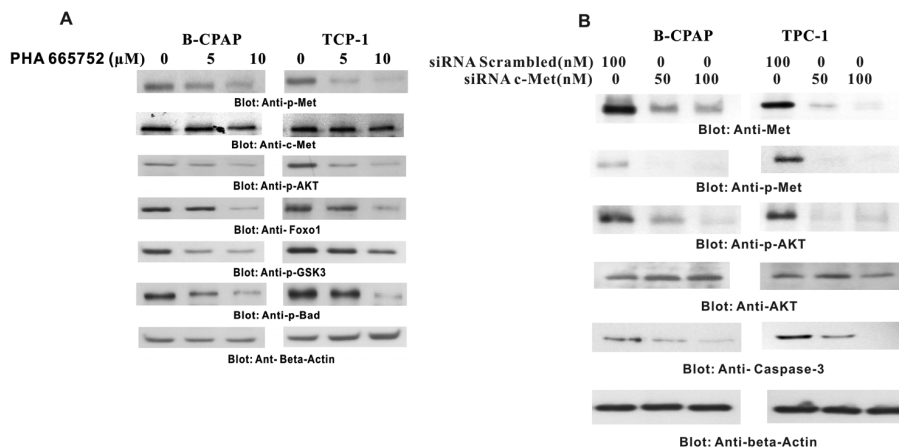
Figure 2. Effect of PHA665752 treatment on c-Met and its downstream signaling pathway. (A) B-CPAP and TPC-1 cells were treated with various doses of PHA665752 as indicated and cytoplasmic extracts were prepared; 10 μg of protein from each sample was separated on SDS-PAGE, transferred to a PVDF membrane and immunoblotted with antibodies against total Met, p-Met, p-AKT, Foxo1, p-GSK3 and p-Bad. The blots were probed with an antibody against β-actin for equal loading. (B) B-CPAP and TPC-1 cells were transfected with scrambled siRNA (100 nmol/L) and c-Met siRNA (50 and 100 nmol/L) for 48 h. After 48 h, cells were lysed and proteins were immunoblotted with antibodies against c-Met, p-Met, AKT, p-AKT, caspase-3 and β-actin.

PHA665752 at doses up to 5 and 10 μmol/L induced apoptosis in malignant pleural mesothelioma cell lines and ovarian carcinoma cell lines via the c-Met pathway, respectively (29,30).

We then examined whether PHA665752 also inhibited p-Met and deregulated downstream components of the c-Met signaling pathway in PTC cells. As shown in Figure 2A, all PTC cell lines expressed constitutive p-Met and p-AKT, and 24 h of treatment with PHA665752 dephosphorylated constitutive p-Met and p-AKT in a dose-dependent manner. Inhibition by PHA665752 further caused inactivation of p-Foxo1, p-GSK3 and p-Bad (Figure 2A). In addition, PHA665752 treatment downregulated the expression of the antiapoptotic genes *XIAP* and *cIAP1* (Figure 3D), suggesting that PHA665752 induces apoptosis in PTC cell lines via inactivation of p-Met activity and deregulation of its downstream substrates.

PHA665752-induced apoptosis via the c-Met signaling pathway was further confirmed in B-CAPA1 cells by transfection studies with two siRNAs specifically targeting different sequences of c-Met. As shown in Figure 2B, c-Met siRNA inhibited c-Met expression, decreased phosphorylation of Met and AKT and downregulated caspase 3. Similar results were obtained by using another c-Met siRNA (data not shown). There results clearly supported the link between c-Met and XIAP/cIAP through AKT phosphorylation in the growth and survival of PTC cells

PHA665752 Induces Apoptosis via Mitochondrial Pathway

Inactivation of Bad has been shown to activate the mitochondrial apoptotic pathway by allowing Bad protein to translocate to mitochondria, leading to conformational changes and upregulation of proapoptotic Bax (31). As shown in Figure 2A, inactivation of AKT leads to dephosphorylation of Bad. We therefore tested the activation of Bax in response to PHA665752 treatment. As shown in Figure 3, inhibition of c-Met resulted in conformational changes and activation of Bax protein starting at 4 and 8 h of PHA665752 treatment. We

then examined the effect of PHA665752 on mitochondrial membrane potentials in those cells. Treatment of PTC cells with PHA665752 led to loss of mitochondrial membrane potential as measured by JC1 stained red fluorescence depicting apoptotic cells (Figure 3B). We further examined cytochrome c release from mitochondria into cytosol in PTC cells treated with PHA665752 for 24 h by Western blotting analysis. Higher levels of cytochrome c were measured in cytosol after PHA665752 treatment (Figure 3C).

PHA665752-Induced ROS Generation Regulates Upregulation of DR5

It has been shown that a number of compounds generate ROS-induced cell death (32), and DR5 expression is upregulated by ROS (33). A recent study conducted by our group demonstrated that PHA665752 induces DR5 upregulation through generating ROS in lymphoma cells (24). We therefore sought to examine whether PHA665752 also generated ROS in PTC cells. H^2DCFDA-based FACS detection revealed that intracellular ROS levels increased in a time-dependent manner in PTC cell lines following treatment with 10 μmol/L PHA665752 (Supplementary Figure 4A), starting as early as 2 h after treatment. To confirm whether PHA665752 generated ROS in PTC cells, we pretreated PTC cells with 10 mmol/L NAC, a scavenger of ROS, for 2 h followed by treatment of PHA665752 for various time periods. Pretreatment with NAC inhibited PHA665753-generated ROS in PTC cells (Supplementary Figure 4B). We then explored whether PHA665752-generated free radicals modulate expression of DR5 in PTC cells. As shown in Figure 4A, PHA665752 treatment of PTC cells upregulated DR5, starting at 3 h. To further confirm whether ROS generation is directly related to PHA665752-induced DR5 upregulation, we examined DR5 expression at the transcriptional and translational levels in PTC cell lines pretreated with 10 mmol/L NAC for 2 h, followed by treatment with PHA665752
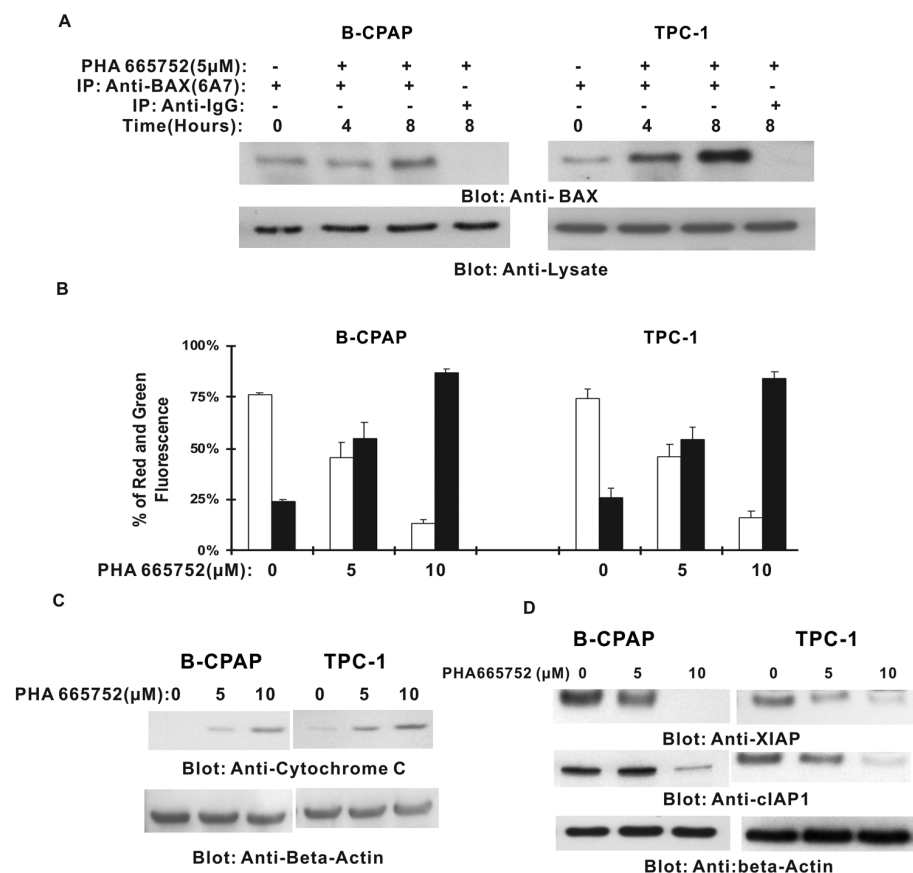
A

B

C

D

Figure 3. PHA665752-induced activation of the mitochondrial apoptosis pathway. (A) Bax conformational change by PHA665752 treatment in PTC cell lines. B-CPAP and TPC-1 cells were treated with 5 μmol/L PHA665752 for 4 and 8 h, respectively; cells were then lysed with 16 mmol/L CHAPS lysis buffer and immunoblotted with Bax rabbit polyclonal antibody. (B) Loss of mitochondrial membrane potential by PHA665752 treatment in PTC cells. B-CPAP and TPC-1 cells were treated with various doses of PHA665752 as indicated for 24 h. Live cells with intact mitochondrial membrane potential (□) and dead cells with lost mitochondrial potential (■) were measured by JC-1 staining and analyzed by flow cytometry as described in Materials and Methods. (C) PHA665752-induced cytochrome c release from mitochondria. B-CPAP and TPC-1 cells were treated with various doses of PHA665752 as indicated for 24 h. Mitochondria-free cytoplasmic fractions were isolated as described in Materials and Methods. Cell extracts were separated on SDS-PAGE, and immunoblotted with an antibody against cytochrome c and β-actin. (D) B-CPAP and TPC-1 cells were treated with various doses of PHA 665752 as indicated and cytoplasmic extracts were prepared, then 10 μg of protein from each sample was separated on SDS-PAGE, transferred to a PVDF membrane and immunoblotted with antibodies against XIAP and cIAP1. The blots were probed with an antibody against β-actin for equal loading.

for 24 h. As shown in Figure 4B, pretreatment with 10 mmol/L NAC notably inhibited PHA665752-induced DR5 upregulation at the mRNA and protein levels in PTC cells. It was confirmed by another experiment in which a second scavenger of ROS, PEG-SOD (polyethylene glycol-conjugated superoxide dismutase), abrogated PHA665752-induced DR5 upregulation in PTC cells (Supplementary Figure 5). These data suggested that upregulation of DR5 induced by PHA665752 in PTC cells is ROS dependent.

PHA665752 Significantly Magnified Antitumor Effects of TRAIL in PTC Cells

Because PHA665752 causes upregulation of DR5, we sought to determine whether PHA665752-induced apoptosis is DR5 independent. After transfection with DR5 siRNA or scrambled siRNA for 48 h, B-CPAP cells were treated with indicated doses of PHA665752 for 24 h, and then apoptosis status was detected by flow cytometer using Annexin/PI staining. As shown in Figure 4C, no statistically significant difference of apoptosis was observed among different siRNA-transfected cell groups treated with same dose of PHA665752 ($P > 0.05$). These results suggested that PHA665752-induced apoptosis is independent of DR5.

In addition, we examined the role of DR5 in PHA665752-modified apoptosis in PTC cells. We transfected DR5 siRNA and scrambled siRNA to B-CPAP cells, followed by 5 and 10 μmol/L PHA665752 treatment for 24 h. After cell lysis, Western blot was performed. As shown in Figure 4D, depression of DR5 did not affect the PHA665752-induced activation of caspase-3 and PARP. These data suggested that PHA665752-modified DR5 upregulation was not involved in the activation of caspase-3 and PARP induced by PHA665752 in PTC cells.

Because upregulation of DR5 expression was observed in PTC cells treated with PHA665752, and many primary tumors are inherently resistant to TRAIL-mediated apoptosis although TRAIL is a fascinating chemotherapeutic agent for cancer treatment, we sought to examine whether subtoxic doses of PHA665752 sensitize the antitumor effects of TRAIL via upregulation of DR5. After 24 h of treatment with 2.5 μmol/L PHA665752, 2.5 ng/mL TRAIL alone or a combination of those two agents, PTC cells were stained with Annexin V/PI, and analyzed by flow cytometry. As shown in Figure 4E, apoptosis induced by the combination of those agents was significantly higher than that induced by each alone ($P < 0.001$).
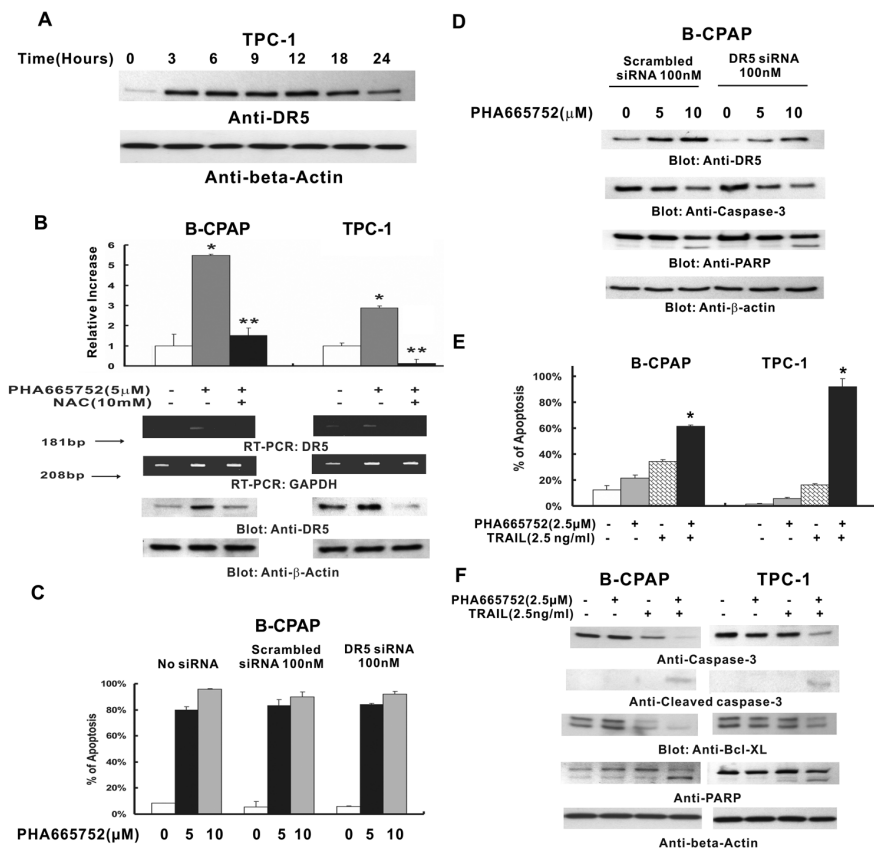
We further explored the underlying mechanism that may be responsible for

Figure 4. Effect of PHA665752 on TRAIL-induced apoptosis in PTC cells. (A) PHA665752 induces upregulation of DR5. TPC-1 cells were treated with 10 μmol/L PHA665752 for the indicated period, then cells were lysed and equal amounts of proteins were separated by SDS-PAGE, transferred to PVDF membrane and immunoblotted with antibodies against DR5. The blots were probed with an antibody against β-actin for equal loading. (B) Effect of NAC on PHA665752-induced DR5 upregulation in PTC cells. B-CPAP and TPC-1 cells were pretreated with 10 mmol/L NAC for 2 h and subsequently treated with 5 μmol/L PHA665752 for 24 h. RT-PCR: total RNA was isolated using Trizol (Invitrogen, Carlsbad, CA, USA) and reverse transcribed with random hexamers. RT-PCR and relative quantification real-time RT-PCR were performed as described in Materials and Methods. Western blot: after cell lysis, equal amounts of proteins were separated by SDS-PAGE, transferred to an immobilon membrane and immunoblotted with antibodies against DR5 and β-actin. *$P < 0.01$ (PHA665752 treatment versus control); **$P < 0.001$ (NAC + PHA665752 treatment versus PHA665752 treatment alone). (C) B-CPAP cells were transfected with or without scrambled siRNA (100 nmol/L) and DR5 siRNA (100 nmol/L) for 48 h. After 48 h, cells were treated with or without indicated doses of PHA665752 for 24 h, and then apoptosis status was detected by flow cytometer using Annexin/PI staining. Columns, mean of three independent experiments; bars, SD. (D) B-CPAP cells were transfected with or without 100 nmol/L scrambled siRNA and 100 nmol/L DR5 siRNA for 48 h. After 2 d, cells were treated with or without indicated doses of PHA665752 for 24 h, then cells were lysed and proteins were immunoblotted with antibodies against DR5, caspase-3, PARP and β-actin. (E) B-CPAP and TPC-1 cells were treated with 2.5 μmol/L PHA665752 alone, 2.5 ng/mL TRAIL alone and two agents in combination for 24 h, and cells were subsequently stained with fluorescein-conjugated Annexin V and propidium iodide and analyzed by flow cytometry. Columns, mean of three independent experiments; bars, SD. *$P < 0.001$. (F) B-CPAP and TPC-1 cells were treated with 2.5 μmol/L PHA665752, 2.5 ng/mL TRAIL and a combination of 2.5 μmol/L PHA665752 with 5 ng/mL TRAIL for 24 h. Then cells were lysed and equal amounts of proteins were separated on SDS-PAGE, transferred to a PVDF membrane and immunoblotted with antibodies against p-Met, caspase 3, cleaved caspase 3, Bcl-XL, PARP and β-actin.

intensification of TRAIL-induced apoptosis by PHA665752. After 24 h of treatment with 2.5 μmol/L of PHA665752, 2.5 ng/mL TRAIL alone, or both in combination, expression of caspase-3, cleaved caspase-3, Bcl-XL and PARP was determined by Western blotting. Only the combination of the two reagents highly affected activation of caspases and PARP cleavage (Figure 4F). These results clearly indicate that PHA665752 enhances TRAIL-induced apoptosis via activation of caspases and cleavage of PARP.

In Vivo Activity of PHA665752 against PTC Cell Xenograft

Our observation that PHA665752 intensifies TRAIL-induced apoptosis in PTC cell lines suggests the potential for therapeutic responses to treatment of PTC. Therefore, we sought to determine whether cotreatment of PHA665752 with TRAIL potentiates the inhibition of PTC xenograft tumors in nude mice. Tumor development and treatment in nude mice were performed as described in Materials and Methods. After 5 wks of treatment, mice were killed and tumors were collected. As shown in Figure 5A, there was significant regression of tumor volume at the end of the fourth week in the group of animals treated with PHA665752 and TRAIL ($P < 0.05$), and the effect was more profound at the end of fifth week ($P < 0.01$). A significant reduction in tumor weight (Figure 5B) was also observed in mice treated with PHA665752 and TRAIL ($P < 0.01$). In addition, images of tumors after necropsy showed that treatment with these two agents resulted in significant shrinkage of tumor size in nude mice (Figure 5C). We further analyzed the status of phosphorylation of c-Met and AKT, and cleavage of caspase-3 and PARP in TPC-1 xenografts with different treatments. As shown in Figure 5D, the levels of p-Met, p-AKT, caspase-3 and PARP were remarkably deceased, and levels of cleaved PARP and caspase-3 were significantly increased in tumors of mice treated with PHA665752 and TRAIL, compared with vehicle,
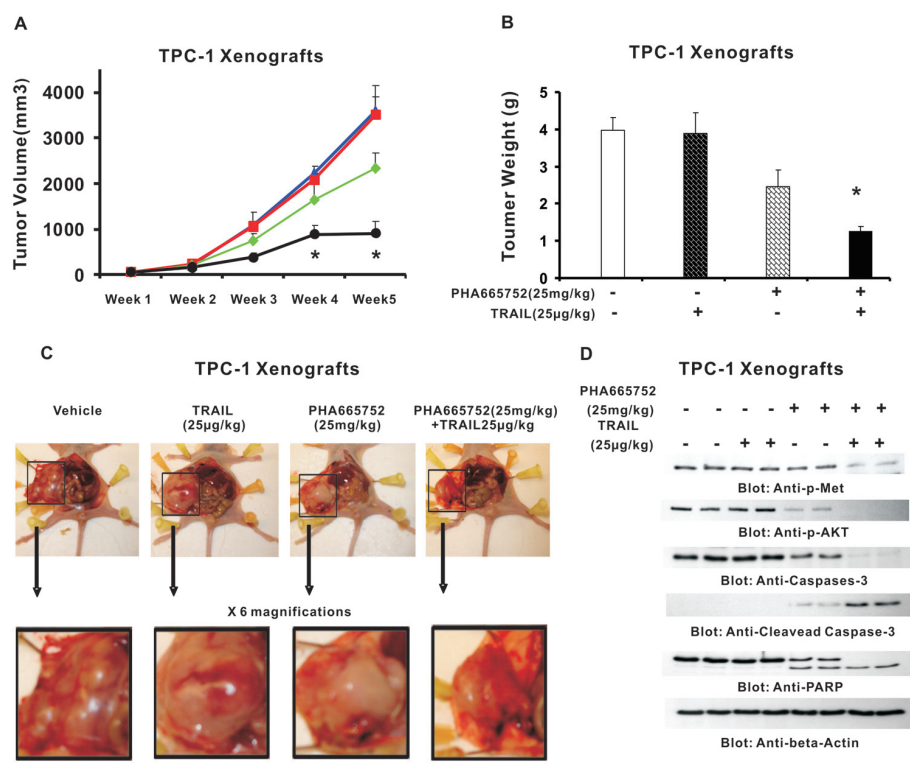
Figure 5. PHA665752 inhibits growth of TPC-1 xenograft and downregulates c-Met and its downstream signaling pathway *in vivo*. Nude mice at 6 wks of age were injected with 10 million MDAH2774 cells. (A) Effect of PHA665752 on TPC-1 xenograft. The volume of each tumor was measured every week. The average (n = 6) tumor volumes in vehicle-treated mice (—▲—) and mice treated with indicated doses of TRAIL (25 µg/kg; —■—), PHA665752 alone (25 µg/kg; —◆—) and a combination of TRAIL and PHA665752 (PHA665752 25 µg/kg + TRAIL 25 µg/kg; —●—) were plotted. The results are expressed as mean ± SD (n = 6). *$P <$ 0.001 compared with vehicle-treated mice. (B) After 5 wks of treatment, mice were killed and tumor weights were measured. The results are expressed as mean ± SD. *$P < 0.001$ compared with vehicle-treated mice by Student *t* test. (C) Representative tumor images of vehicle-treated mice and mice treated with PHA665752 and/or TRAIL after necropsy. (D) Whole cell homogenates from mice treated with vehicle, 25 µg/kg TRAIL, 25 mg/kg PHA665752 and a combination of 25 µg/kg TRAIL and 25 mg/kg PHA665752 were immunoblotted with p-Met, p-AKT, caspase 3, cleaved caspase 3, PARP and β-actin antibodies.

PHA665752 alone and TRAIL alone. Our data indicate that PHA665752 treatment augmented antitumor effects of TRAIL in TPC-1 cell xenografts in nude mice.

DISCUSSION

HGF plays a major role in tumor proliferation, migration, invasion and metastasis via the c-Met pathway in variety of cancers (34,35). The tumorigenic activity of c-Met depends on deregulation of the HGF/c-Met signaling pathway, which results in phosphorylation and activation of AKT (36–38). AKT plays an important role in cell survival and antiapoptosis via modulating the expression of antiapoptotic genes.

Several studies (14,39,40) have previously demonstrated the oncogenic role of c-Met in thyroid carcinogenesis. PTC showing Met expression was associated with an aggressive phenotype characterized by higher stage, nodal involvement, extrathyroidal extension metastasis and tall cell variant histology. Chattopadhyay *et al.* (41) have confirmed the therapeutic rationale of c-Met inhibition by demonstrating that treatment of PHA665752 in-

duced the apoptosis in PTC cell-line cells via cleavage of PARP; this dramatically suppressed invasion and migration induced by HGF.

In the current study, stratification of PTC cases on the basis of expression of p-Met and DR5 led to the identification of an aggressive phenotype (coexpression of p-Met and DR5) that was associated with older age and advanced stage and showed activation of the PI3K/AKT signaling pathway. In an earlier study (42) we had also investigated the role of PI3K/AKT signaling and the RAS–RAF–MEK (mitogen-activated protein kinase/ERK kinase)–ERK (extracellular-signal-regulated kinase) pathway in papillary thyroid carcinomas. *BRAF* mutations were seen in 153 (51.7%) of 296 PTC cases analyzed; *PIK3CA* gene mutations in 4 (1.9%) of 207 PTC cases; and *N2-RAS* mutations in 16 (6%) of 265 PTC cases. We then analyzed the association between *BRAF* mutation and p-Met expression in the PTC subgroup for which data were available for *BRAF* mutations (n = 296). p-Met expression detected by IHC was significantly higher ($P = 0.0194$) in the PTC subgroup with *BRAF* mutation (84.01 ± 66.06) compared with the PTC subgroup that had no *BRAF* mutation (66.14 ± 52.85; data not shown). Interestingly, Kumagai *et al.* (43) have studied the incidence of mutations in *ARAF*, *CRAF* and *MET* genes, and hotspots of *K-RAS* and *N-RAS* genes in Japanese PTC lacking *BRAF* mutations. Because of lack of mutations in these genes in *BRAF*-negative PTC, the authors concluded that that although *ARAF*, *CRAF* and *MET* are actively expressed, alterations of these genes are rare in PTC and unlikely to play a perceptible role in molecular pathogenesis.

PHA665752, an inhibitor of c-Met tyrosine kinase activity, induces dose-dependent inhibition of cell proliferation and induction of apoptosis via the mitochondrial apoptotic pathway in PTC cell lines. PHA665752 also inactivated c-Met and dephosphorylated AKT and its downstream substrates FOXO1, GSK3 and Bad, and downregulated the expression of the

antiapoptotic genes *XIAP* and *cIAP1*. Furthermore, gene silencing of c-Met via its specific siRNA depleted its expression as well as abrogated c-Met–mediated AKT signaling, confirming that PHA665752 specifically induces its apoptotic effect, causing inhibition of cell viability via inactivation of Met and AKT.

Among all the apoptosis-inducing cytokines, TRAIL is the only one still being actively pursued for its anticancer properties in the clinic. Many human cancer cell types, however, are resistant to TRAIL-induced apoptosis (44). Agents that can sensitize tumor cells to TRAIL have great potential for making cancer therapy more effective. In the present study, we explored the role of PHA665752 in upregulation of DR5 leading to sensitization of PTC cells to TRAIL-induced apoptosis. Our data demonstrate that PHA665752 significantly upregulated DR5 expression, thereby allowing TRAIL to effectively induce apoptosis in combination with PHA665752 in PTC cells. Nontoxic doses of PHA665752 and TRAIL also allow PTC cells to undergo efficient apoptosis without causing any weight loss or any visible sickness. Our *in vivo* studies on the effect of PHA665752 and TRAIL on growth of PTC cell tumors in a murine xenograft model are consistent with results obtained from *in vitro* cell line data. In addition to an overall significant regression of tumor volume and loss of tumor weight following treatment with PHA665752 and TRAIL, Western blotting analysis of tumors also showed remarkable decreased c-Met and AKT activity, and cleavage of caspase-3 and PARP in mice treated with subtoxic dose of PHA665752 and TRAIL.

The current study expands on our earlier findings of an oncogenic role of Met signaling in PTC. We have demonstrated that inhibition of c-Met by PHA665752 causes apoptosis via the mitochondrial apoptotic pathway, and PHA665752 also synergizes death receptor–induced apoptosis via upregulation of DR5, suggesting the combination of PHA665752 and TRAIL may be a novel strategy for the treatment of PTC and other human cancers that are resistant to chemotherapy.

We hypothesize that molecular profiling on the basis of p-Met and DR5 expression could lead to the identification of a subset of primary PTCs and, more importantly, recurrent/metastatic PTCs that are resistant to conventional therapy. Such recurrent/metastatic lesions usually have dysregulated Met signaling and could be targeted with newer drugs. Further validation and additional studies could provide new vistas for treatment of recurrent cases of PTC that are generally refractory and resistant to therapy.

In summary, our data indicate that high coexpression of p-Met and DR5 is linked to activation of PI3K/AKT and associated with aggressive phenotypes in Middle Eastern PTC; inhibition of c-Met by PHA665752 causes apoptosis via the mitochondrial apoptotic pathway and PHA665752 also synergizes death receptor–induced apoptosis via upregulation of DR5. These findings suggest that the combination of PHA665752 and TRAIL may be a novel strategy for the treatment of refractory PTC.

DISCLOSURE

The authors declare that they have no competing interests as defined by *Molecular Medicine*, or other interests that might be perceived to influence the results and discussion reported in this paper.

REFERENCES

1. Nikiforov YE. (2008) Thyroid carcinoma: molecular pathways and therapeutic targets. *Mod. Pathol.* 21(Suppl 2):S37–43.
2. Piersanti M, Ezzat S, Asa SL. (2003) Controversies in papillary microcarcinoma of the thyroid. *Endocr. Pathol.* 14:183–91.
3. Loh KC, Greenspan FS, Gee L, Miller TR, Yeo PP. (1997) Pathological tumor-node-metastasis (pTNM) staging for papillary and follicular thyroid carcinomas: a retrospective analysis of 700 patients. *J. Clin. Endocrinol. Metab.* 82:3553–62.
4. Hay ID. (1990) Papillary thyroid carcinoma. *Endocrinol. Metab. Clin. North Am.* 19:545–76.
5. Siironen P, *et al.* (2005) Prognostic factors in papillary thyroid cancer: an evaluation of 601 consecutive patients. *Tumour Biol.* 26:57–64.
6. Gonzatti-Haces M, *et al.* (1988) Characterization of the TPR-MET oncogene p65 and the MET protooncogene p140 protein-tyrosine kinases. *Proc. Natl. Acad. Sci. U. S. A.* 85:21–5.
7. Bardelli A, Ponzetto C, Comoglio PM. (1994) Identification of functional domains in the hepatocyte growth factor and its receptor by molecular engineering. *J. Biotechnol.* 37:109–22.
8. Lesko E, Majka M. (2008) The biological role of HGF-MET axis in tumor growth and development of metastasis. *Front. Biosci.* 13:1271–80.
9. Desiderio MA. (2007) Hepatocyte growth factor in invasive growth of carcinomas. *Cell. Mol. Life Sci.* 64:1341–54.
10. Tulasne D, Foveau B. (2008) The shadow of death on the MET tyrosine kinase receptor. *Cell. Death Differ.* 15:427–434.
11. Mineo R, *et al.* (2004) Activation of the hepatocyte growth factor (HGF)-Met system in papillary thyroid cancer: biological effects of HGF in thyroid cancer cells depend on Met expression levels. *Endocrinology.* 145:4355–65.
12. Ruco LP, Stoppacciaro A, Ballarini F, Prat M, Scarpino S. (2001) Met protein and hepatocyte growth factor (HGF) in papillary carcinoma of the thyroid: evidence for a pathogenetic role in tumourigenesis. *J. Pathol.* 194:4–8.
13. Wasenius VM, Hemmer S, Kettunen E, Knuutila S, Franssila K, Joensuu H. (2003) Hepatocyte growth factor receptor, matrix metalloproteinase-11, tissue inhibitor of metalloproteinase-1, and fibronectin are up-regulated in papillary thyroid carcinoma: a cDNA and tissue microarray study. *Clin. Cancer Res.* 9:68–75.
14. Siraj AK, *et al.* (2007) Genome-wide expression analysis of Middle Eastern papillary thyroid cancer reveals c-MET as a novel target for cancer therapy. *J. Pathol.* 213:190–9.
15. Bauer J, Wekerle H, Lassmann H. (1995) Apoptosis in brain-specific autoimmune disease. *Curr. Opin. Immunol.* 7:839–43.
16. Ghobrial IM, Witzig TE, Adjei AA. (2005) Targeting apoptosis pathways in cancer therapy. *C. A. Cancer J. Clin.* 55:178–94.
17. Bavi P, *et al.* (2006) Prevalence of fragile histidine triad expression in tumors from Saudi Arabia: a tissue microarray analysis. *Cancer Epidemiol. Biomarkers Prev.* 15:1708–18.
18. Uddin S, *et al.* (2008) Fatty acid synthase and AKT pathway signaling in a subset of papillary thyroid cancers. *J. Clin. Endocrinol. Metab.* 93:4088–97.
19. Uddin S, *et al.* (2006) Role of phosphatidylinositol 3′-kinase/AKT pathway in diffuse large B-cell lymphoma survival. *Blood.* 108:4178–86.

20. Abubaker J, *et al.* (2008) Clinicopathological analysis of colorectal cancers with PIK3CA mutations in Middle Eastern population. *Oncogene.* 27:3539–45.

21. Mandal M, *et al.* (2005) The Akt inhibitor KP372–1 suppresses Akt activity and cell proliferation and induces apoptosis in thyroid cancer cells. *Br. J. Cancer.* 92:1899–905.

22. Hussain AR, *et al.* (2006) Curcumin induces apoptosis via inhibition of PI3′-kinase / AKT pathway in acute T cell leukemias. *Apoptosis.* 11:245–54.

23. Uddin S, Hussain A, Al-Hussein K, Platanias LC, Bhatia KG. (2004) Inhibition of phosphatidylinositol 3′-kinase induces preferentially killing of PTEN-null T leukemias through AKT pathway. *Biochem. Biophys. Res. Commun.* 320:932–8.

24. Hussain AR, *et al.* (2007) Sanguinarine-dependent induction of apoptosis in primary effusion lymphoma cells. *Cancer Res.* 67:3888–97.

25. Uddin S, Ah-Kang J, Ulaszek J, Mahmud D, Wickrema A. (2004) Differentiation stage-specific activation of p38 mitogen-activated protein kinase isoforms in primary human erythroid cells. *Proc. Natl. Acad. Sci. U. S. A.* 101:147–52.

26. Uddin S, *et al.* (2005) Inhibition of phosphatidylinositol 3′-kinase / AKT signaling promotes apoptosis of primary effusion lymphoma cells. *Clin. Cancer Res.* 11:3102–8.

27. Christensen JG, Burrows J, Salgia R. (2005) c-Met as a target for human cancer and characterization of inhibitors for therapeutic intervention. *Cancer Lett.* 225:1–26.

28. Tjin EP, *et al.* (2006) Functional analysis of HGF / MET signaling and aberrant HGF-activator expression in diffuse large B-cell lymphoma. *Blood.* 107:760–8.

29. Bu R, *et al.* (2011) HGF / c-Met pathway has a prominent role in mediating antiapoptotic signals through AKT in epithelial ovarian carcinoma. *Lab. Invest.* 91:124–37.

30. Mukohara T, *et al.* (2005) Inhibition of the met receptor in mesothelioma. *Clin. Cancer Res.* 11:8122–30.

31. Samovski D, Kalderon B, Yehuda-Shnaidman E, Bar-Tana J. (2010) Gating of the mitochondrial permeability transition pore by long chain fatty acyl analogs in vivo. *J. Biol. Chem.* 285:6879–90.

32. Chou WC, Dang CV. (2005) Acute promyelocytic leukemia: recent advances in therapy and molecular basis of response to arsenic therapies. *Curr. Opin. Hematol.* 12:1–6.

33. Jung EM, Lim JH, Lee TJ, Park JW, Choi KS, Kwon TK. (2005) Curcumin sensitizes tumor necrosis factor-related apoptosis-inducing ligand (TRAIL)-induced apoptosis through reactive oxygen species-mediated upregulation of death receptor 5 (DR5). *Carcinogenesis.* 26:1905–13.

34. Ma PC, Maulik G, Christensen J, Salgia R. (2003) c-Met: structure, functions and potential for therapeutic inhibition. *Cancer Metastasis Rev.* 22:309–25.

35. Furge KA, Zhang YW, Vande Woude GF. (2000) Met receptor tyrosine kinase: enhanced signaling through adapter proteins. *Oncogene.* 19:5582–9.

36. Sawada K, *et al.* (2007) c-Met overexpression is a prognostic factor in ovarian cancer and an effective target for inhibition of peritoneal dissemination and invasion. *Cancer Res.* 67:1670–9.

37. Koon EC, *et al.* (2008) Effect of a c-Met-specific, ATP-competitive small-molecule inhibitor SU11274 on human ovarian carcinoma cell growth, motility, and invasion. *Int. J. Gynecol. Cancer.* 18:976–84.

38. Xiao GH, Jeffers M, Bellacosa A, Mitsuuchi Y, Vande Woude GF, Testa JR. (2001) Anti-apoptotic signaling by hepatocyte growth factor / Met via the phosphatidylinositol 3-kinase / Akt and mitogen-activated protein kinase pathways. *Proc. Natl. Acad. Sci. U. S. A.* 98:247–52.

39. Chen BK, *et al.* (1999) Overexpression of c-Met protein in human thyroid tumors correlated with lymph node metastasis and clinicopathologic stage. *Pathol. Res. Pract.* 195:427–33.

40. Ramirez R, *et al.* (2000) Over-expression of hepatocyte growth factor / scatter factor (HGF / SF) and the HGF / SF receptor (cMET) are associated with a high risk of metastasis and recurrence for children and young adults with papillary thyroid carcinoma. *Clin. Endocrinol.* 53:635–44.

41. Chattopadhyay C, El-Naggar AK, Williams MD, Clayman GL. (2008) Small molecule c-MET inhibitor PHA665752: effect on cell growth and motility in papillary thyroid carcinoma. *Head Neck.* 30:991–1000.

42. Abubaker J, *et al.* (2008) Clinicopathological analysis of papillary thyroid cancer with PIK3CA alterations in a Middle Eastern population. *J. Clin. Endocrinol. Metab.* 93:611–8.

43. Kumagai A, *et al.* (2006) No evidence of ARAF, CRAF and MET mutations in BRAFT1799A negative human papillary thyroid carcinoma. *Endocr. J.* 53:615–20.

44. Zhang L, Fang B. (2005) Mechanisms of resistance to TRAIL-induced apoptosis in cancer. *Cancer Gene. Ther.* 12:228–37.